

# Radiation test of a BLDC motor driver component

Sedlmayr Hans-Juergen<sup>a</sup>, Beyer Alexander<sup>a</sup>, Kunze Klaus<sup>a</sup> and Maier Maximilian<sup>a</sup>

**Abstract**—Robotic systems will become in the future of space exploration an important technology, whereby brushless motor drives are used for locomotion and manipulation. This paper presents the radiation test results of a COTS motor driver.

**Index Terms**—radiation, test, BLDC, motor, driver, space, robotic

## I. INTRODUCTION

New robotic systems for space applications like the Spacehand [1], [2] or the CAESAR (Compliant Assistance and Exploration Space Robot) robotic arm are highly integrated mechatronic systems. Due to the high number of parts which must be integrated to operate such systems, the remaining space for the integration is pretty low. Fig. 1 shows the four finger DEXHAND which was developed for on-orbit servicing applications on the ISS. Furthermore remote acting landers like MASCOT [3], [4] (Mobil Asteroid Surface Scout) or rovers like LRU [5] (Lightweight Rover Unit) are designed to have a small form factor in order to reduce weight and therefore reduce costs for launch. Most of these applications could be locomoted by using of a flexible three phase BLDC motor driver unit [6]. This unit was newly developed by DLR-RM in order to satisfy the increasing demand on compact driver stages on the one hand. On the other hand, the development effort for different systems could be dramatically minimized based on re-usage of flexible standard components. The radiation requirements for all these missions allow the use of medium radiation tolerant systems which could be realized by a partial spin-in of automotive or military rated components. The spin-in of automotive rated COTS parts is a good option due to the extended storage temperature range of approx.  $-55^{\circ}\text{C}$  up to  $150^{\circ}\text{C}$  and the operating temperature range of approx.  $-40^{\circ}\text{C}$  up to  $125^{\circ}\text{C}$ . These specifications are close to the space grade temperature range which minimize the effort of the up-screening. In addition,

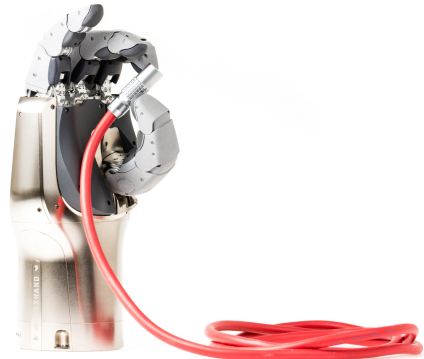


Figure 1. DEXHAND with a pinch grasp

the number of parts being delivered to customers is usually rather high, therefore the manufacturer has a good overview on the quality of the produced parts. Based on these facts, a Three Phase PWM Motor Driver DRV8332 from TI was tested as possible flight candidate. This integrated high performance three phase motor driver consists of 6 integrated power MOSFETS with a low resistance, allows up to 8A continuous phase current (13A peak) in an ambient operating temperature of up to  $85^{\circ}\text{C}$  and consists of several integrated security features such as an over current detection. More details on this driver could be found on TI's website [7]. To get a full picture of the radiation performance a total ionizing dose (TID) test, a proton test and a heavy ion test was conducted.

## II. ENVIRONMENT

The successor of the DEXHAND - the so called Spacehand [2] must be able to survive a multiple year mission in geosynchronous Orbit (GEO) in order to meet the requirements of the RSGS mission (Robotic Servicing of geosynchronous Satellites) of DARPA [8], NRL [9] and SSL [10]. These needs define the most challenging requirements for the next upcoming missions at our institute. The upper limit of the total dose was set to 500 Gy(Si), which was the limit of some radiation tolerant parts in our systems, too.

<sup>a</sup>is with Institute of Robotics and Mechatronics (RM), German Aerospace Center (DLR), Muenchener Str. 20, 82234 Wessling, Germany  
Email: Hans-Juergen.Sedlmayr@dlr.de, Phone: +49(0)8153-28-3532

A radiation analysis based on a 10 year mission in GEO (without transfer orbit) was performed with ESA's SPENVIS (Space Environment Information System) [11] tool chain. The total ionizing dose was estimated by the usage of the Shieldose-2 model [12] for simple geometries. Fig. 2 shows the result of the different simulation runs which differ in the material of the shielding and the shield configuration. Obviously a housing thickness between 2.5 mm and 5.5 mm must be used to reach the 500 Gy(Si) limit, depending on the material and the shielding configuration. During the further procedure a 3 mm Aluminium housing was used as baseline.

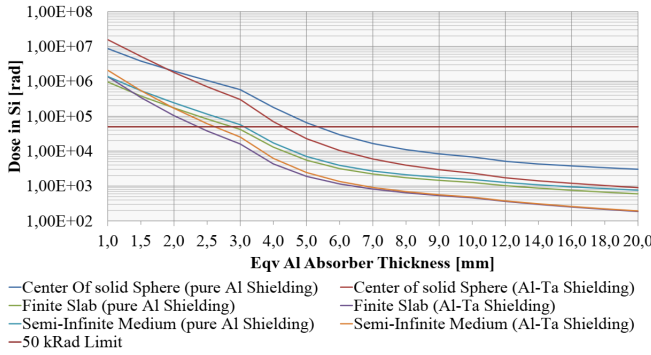


Figure 2. Total ionizing dose vs. equivalent shielding Al absorber thickness for different materials and shielding configuration

Fig. 3 shows the long-term shielded LET spectra based on trapped protons (AP-9 model, [13]), solar particles (ESP-PSYCHIC, H - Ni) and galactic cosmic rays particles (ISO 15390 GCR, H - Ni) [14] behind the 3 mm Aluminium housing.

The different radiation tests were performed according to the basic specification ESCC 25100 [15], ESCC 22900 [16], ESCC 23100 [17] provided by the European Space Components Coordination (ESCC, [18]) and the standard ECSS-Q-60-13C [19] provided by the European Cooperation for Space Standardization (ECSS, [20]). The limits were chosen with respect to the simulation results.

The TID test was performed at the Helmholtz Zentrum Berlin Wannsee (HZB) [21] with biased samples and a dose rate of 3.82 Gy(Si)/hour ('Standard Rate') up to 550 Gy(Si). During the irradiation some important parameter were monitored in-situ with a specially designed test hardware. Similar to the TID test, a proton test was performed at the HZB, too. Hereby a fluence of 1.7E+10 protons per square centimetre was applied. Three different energies were used for this campaign: 30 MeV, 50 MeV and 68 MeV per proton.

Finally a heavy ion test was performed at the radiation

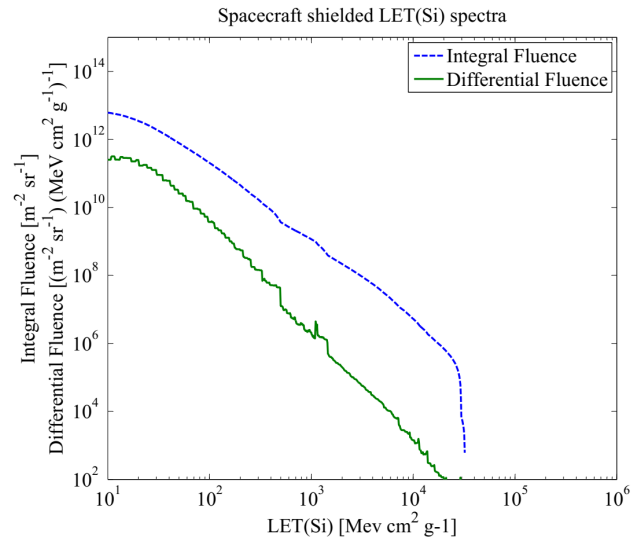


Figure 3. Long-term shielded LET spectra for 10 year GEO mission

effects facility in Jyvaskyla (RADEF) [22], where Nitrogen, Krypton and Xenon ions were used. The applied fluence was 1.0E+10 ions per square centimetre for each ion species.

### III. TOTAL DOSE RESPONSE

During the TID test at room temperature a running brushless DC (BLDC) motor was used as load for the DRV8332 output stages and the motor rotation was monitored by a reference encoder. All measured data were collected by the radiation test motherboard (RTM), an multiple purpose test board which was developed by DLR-RM. This board is able to stimulate and interface multiple clients by means of test specific interface boards (IF) which are used to adapt voltages for instance or to provide additional control logic if needed. Fig. 4 shows four RTM-IF stacks mounted on a backplane used for the DRV8332 radiation test campaigns.

To operate the DRV8332 with a rotating BLDC motor as load, multiple digital I/O lines and PWM signals are needed. In addition, the needed commutation logic must be provided, since the DRV8332 has no capability to make a motor rotate by oneself. This was done by a so called six-step-commutation where one mechanical rotation is divided in six sectors which could be reached by controlling the three PWM output voltages accordingly. All these measurements were realised by a small FPGA on the interface board.

The monitored parameter were measured by multiple ADCs. These data and all needed digital status information were sent to the test control PC which is located

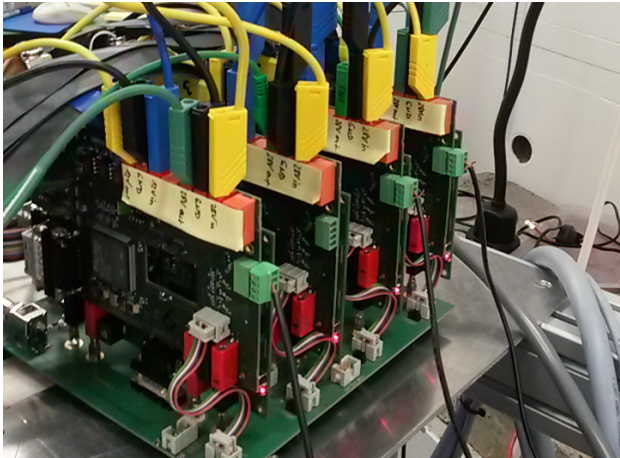


Figure 4. *Radiation test motherboard (RTM)*

outside the test chamber by means of a serial interface. This interface could be used to control the test flow or to switch the power supplies on or off. A block diagram of the test setup is shown in Fig. 5. This setup was used for all tests which were conducted within this campaign. During the test procedure the input currents of both

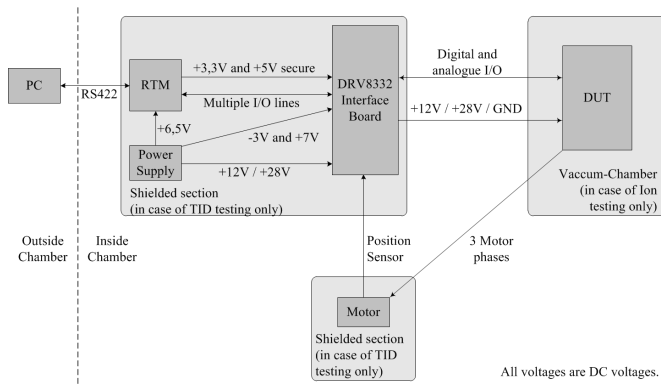


Figure 5. *Block diagram of the DRV8332 test setup*

supply voltages, some pin input currents and the status flags of the DRV8332 were monitored permanently. The motor was alternately operated and stopped during the test procedure depending on the parameter which were measured or on the functionality which was tested. A simplified schematic test flow is depicted in Fig. 6. The test ended when the total dose was reached or a severe error was detected.

For an increased clarity of the plots within this chapter, every 100 Gy a subset of the data was taken and printed, unless otherwise noted. The color coding represents the different samples which were irradiated.

Fig. 7 shows the 12V digital supply current over dose

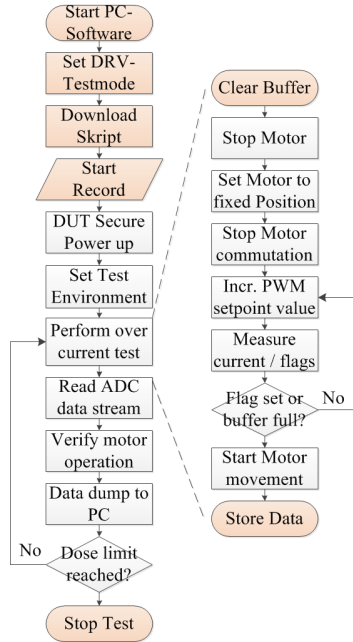


Figure 6. *Test flow of the DRV8332 TID test*

at room temperature. The variation of the supply currents at one dose step represents the different operating modes during the test. Due to the huge compression of the x-axis, the curves are displayed as dots. Although the supply current increased clearly visible, the supply current was within the maximum ratings at the end of the TID test.

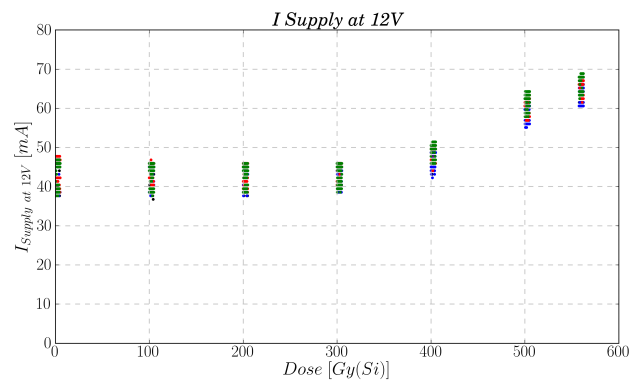


Figure 7. *Digital supply current (12V) over dose*

Of course, the 28V motor supply current was measured, too. During the recording no TID based effects were measured which means that the built in MOSFETs worked without any major degradation.

The DRV8332 offers a built in voltage regulator which provides suitable voltage levels for the digital and low-

voltage analogue circuitry. This output was measured, too and the results are plotted in Fig. 8. At the end of the TID test, the output voltage was within the rated values.

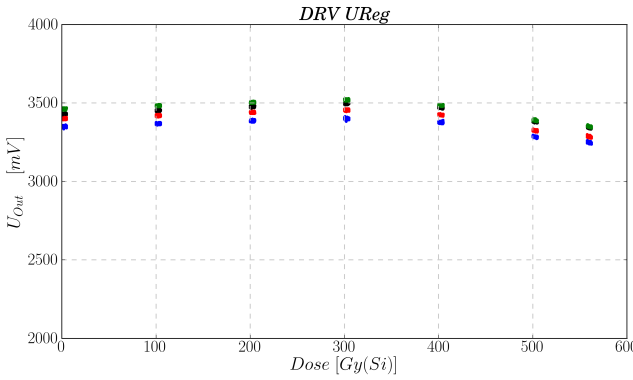


Figure 8. Voltage regulator output voltage over dose

Finally the in- and output-currents of several I/O pins were measured during the irradiation. Hereby we measured two different behaviours. The open drain outputs for error indication kept their driving capability without major differences while the leakage current of the mode selection pin input M1 increased with increasing dose. Fig. 9 shows the recorded behaviour. The negative sign of the current indicates that the pin acted as source during the measurement.

The DUT offers a build-in motor current limitation with

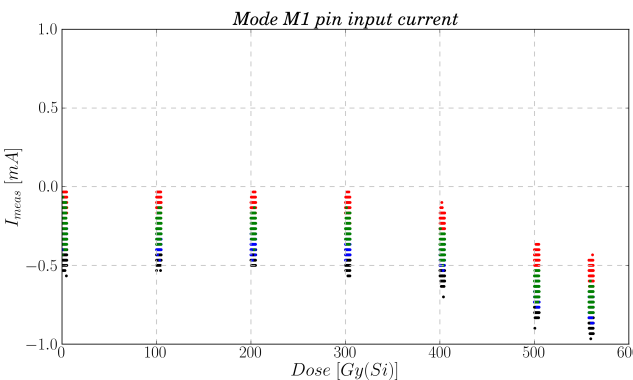


Figure 9. Leakage current of the mode selection pin M1

a cut-off functionality based on an external shunt resistor for each of the three phases. This threshold was verified when the rotation of the motor was stopped with an increasing PWM setpoint value which leads to an rising current through the motor until the DUT cuts off the motor current. The interruption of the motor rotation was

necessary in order to verify each of the motor phases independently. The principle of this subtest is plotted in the right tree of the test flow which is depicted in Fig. 6. During this subtest, the motor current was permanently sampled and recorded with 40 kHz. The results are plotted exemplarily for motor position 'Hall 6' in Fig. 10 over dose and time.

In the figure, the x-axis contains samples which corresponds to the recorded data with a resolution of 25 us per sample. In total the plotted 35 samples corresponds to 875 us test time. The z-axis contains the dose steps which were selected for plotting. And finally the y-axis contains the supply current in mA.

In conclusion at the end of the total ionizing test, all

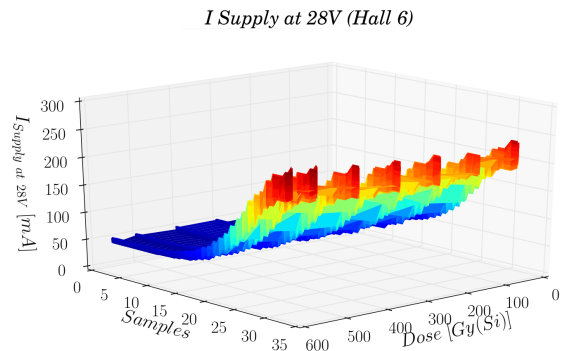


Figure 10. Motor supply current (28V) over time and dose during over current cut-off testing

measured parameters stayed within their maximum limits up to 550 Gy(Si).

#### IV. SINGLE EVENT TESTING

During the proton and heavy ion test, the same test setup and test principle was used as during the TID test. The irradiation with protons resulted in a few smaller upsets which could be measured at the in- and output-currents of the pins. No further severe effects could be measured.

As an example, the output current of the OTW pin is plotted in Fig. 11. Similar to the plots in the last chapter, the colors of the curves define the different samples. But contrary to the dose information, the beam time is used as x-axis. In order to have a compact plot, all test sections with the different particle energies (proton beam) or the used particles (heavy ion beam) are concatenated. The start of each section is indicated by a coloured vertical dotted line.

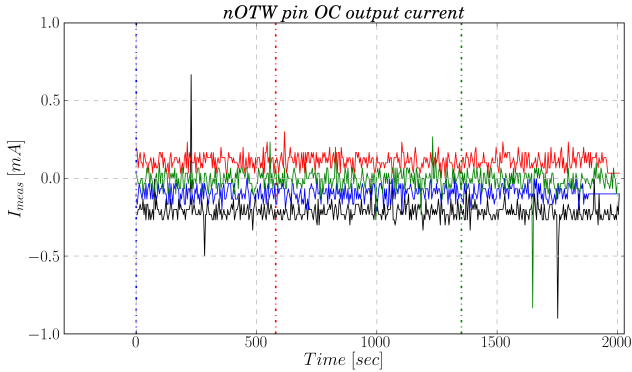


Figure 11. OTW pin output current during proton irradiation

Although several peaks could be measured in the output current of the OTW pin, the output voltage was stable all over the time. The following figure Fig. 12 shows the digital interpretation of the OTW pin output voltage which was regularly read by a digital I/O port of the RTM.

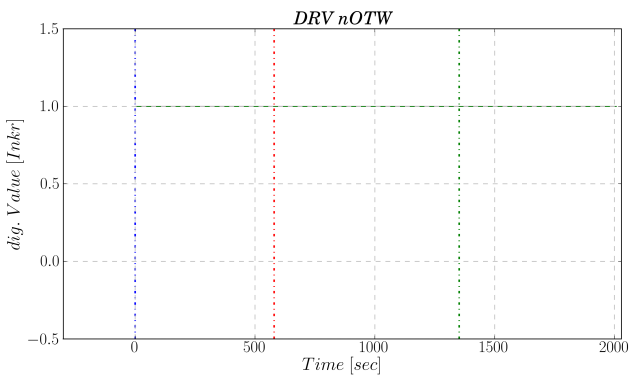


Figure 12. OTW pin output voltage during proton irradiation

Finally figure Fig. 13 shows the output of the used resolver where the motor movement was monitored during the test. Since no active speed control loop was active during the test campaign, the rotational speed is a bit noisy which is due to the non constant mechanical properties of the test bench (e.g. friction).

The noise on the resolver output signal is not a criteria for finding radiation based effects. Only when an unintentionally standstill of the motor would be indicated, which was not the case during the proton test campaign, a radiation based effect could be the reason.

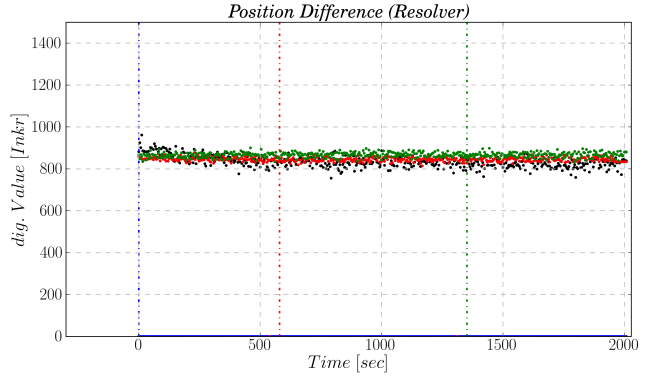


Figure 13. motor movement measured by a resolver during proton irradiation

For the heavy ion test the DUTs were delidded by chemical etching. That means that the thermal heat sink of the chip (metal plate on the package) was removed, too. To avoid parasitic effects due to the missing heat distribution capability and due to the fact that the test was conducted in a vacuum chamber, the load was reduced and the ambient temperature was kept at room temperature. The following table Tab. I gives an overview of the different used ion species and the corresponding LET values which were archived partly by tilting of the DUT during the irradiation.

Up till a LET of  $52.9 \text{ MeV} \cdot \text{cm}^2/\text{mg}$  no severe effect

Table I  
Used ion species and their LET values

Ion species	LET value [ $\text{MeV} \cdot \text{cm}^2/\text{mg}$ ]
Nitrogen	1.89
Nitrogen	3.80
Krypton	40.0
Krypton	52.9
Xenon	59.9

could be measured. But during the next irradiation step with a LET of  $59.9 \text{ MeV} \cdot \text{cm}^2/\text{mg}$  the DRV8332 stopped its operation due to a partial latch-up of the internal control electronics. This latch-up could be seen in Fig. 14 where the 12V supply voltage was analogue sampled and plotted over time exemplarily for motor position 'Hall 2'. The plotting and data recording principle is identically to the motor supply current which was depicted in Fig. 10 in the last chapter with the exception that the z-axis contains the increasing test time instead of the dose values.

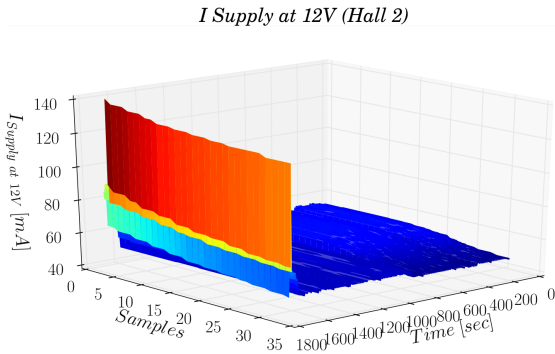


Figure 14. 12V supply current during heavy ion irradiation over time

During the last irradiation step (which is shown on the left side of Fig. 14), the high current phase was triggered by the ions and lasted over several milliseconds. Therefore the current decrease is not visible within the plotted 875 us. During the next program iteration which was performed by the RTM, the high current phase was already cleared and the supply current returned to a lower plateau, but not to the original level which is indicated in the figure by the different intensities of the blue color. During this self clearing event, the 28V motor supply current was slightly higher compared to the normal operation, but no excessive over current could be measured, which is depicted in Fig. 15. This points to a still working shot-through protection as well as a working short-circuit protection of the DRV8332.

Besides the monitoring of the over temperature warn-

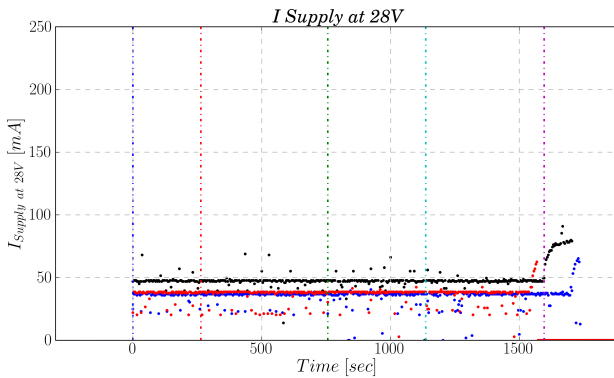


Figure 15. 28V supply current during heavy ion irradiation over time

ing pin (OTW), the temperature of the DRV8332 was measured by the RTM, too. The OTW signal was not triggered during the latchup event due to the low energy

and the short duration of the over current phase. This point to the fact that the internal temperature was below 115 °C.

The results of the temperature measurements are shown in Fig. 16. It's clearly visible that the temperature of the DRV8332 stabilizes during each irradiation step after a short warm up phase. Only during the latchup event the temperature of the DRV8332 was slightly increased compared to the preceding temperature niveaus due to the higher current load in the protection and I/O logic block.

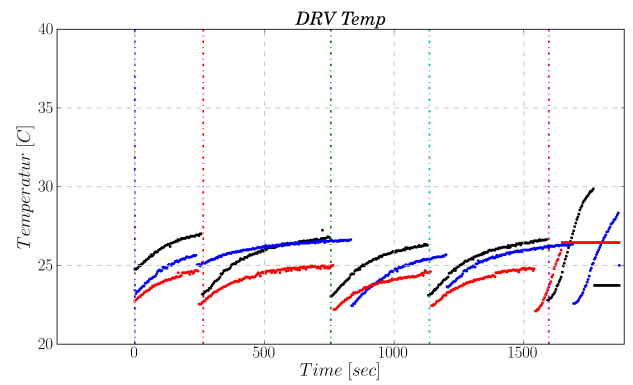


Figure 16. Temperature reading during heavy ion irradiation over time

## V. CONCLUSION

This paper presented the characterisation of the radiation performance of the Three Phase PWM Motor Driver DRV8332 from TI. With respect to intended mission and the required TID performance of 500 Gy(Si) the DUT performed well. The latch-up threshold LET of the device could be found at  $59.9 \text{ MeV} \cdot \text{cm}^2/\text{mg}$ . This is an acceptable value, since the statistics of the operation time during the mission lowers the risk of an error immense.

## VI. ACKNOWLEDGMENT

This work was funded by DLR-RM and the Government of Bavaria. The authors would like to thank the electronics team at DLR-RM for their help during the development and production of the needed test electronics.

## REFERENCES

- [1] M. Chalon, M. Maier, A. Bertleff, W. and Beyer, R. Bayer, W. Friedl, P. Neugebauer, T. Obermeier, H.-J. Sedlmayr, N. Seitz, and A. Stemmer, "SPACEHAND: a multi-fingered robotic hand for space," in *13th Symposium on Advanced Space Technologies in Robotics and Automation (ASTRA)*, ESA/ESTEC, Noordwijk, Netherlands, May 2015.

- [2] A. Wedler, M. Chalon, A. Baumann, W. Bertleff, A. Beyer, R. Burger, J. Butterfass, M. Grebenstein, R. Gruber, F. Hacker, E. Krämer, K. Landzettel, M. Maier, H.-J. Sedlmayr, N. Seitz, F. Wappeler, B. Willberg, T. Wimböck, F. Didot, and G. Hirzinger, “DLR’s space qualifiable multi-figered DEXHAND,” in *11th Symposium on Advanced Space Technologies in Robotics and Automation (ASTRA)*, ESA/ESTEC, Noordwijk, Netherlands, April 2011.
- [3] J. Reill, H.-J. Sedlmayr, P. Neugebauer, M. Maier, E. Krämer, and E. Lichtenheldt, “MASCOT - Asteroid Lander with innovative Mobility Mechanism,” in *13th Symposium on Advanced Space Technologies in Robotics and Automation (ASTRA)*, ESA/ESTEC, Noordwijk, Netherlands, May 2015.
- [4] T.-H. Ho, V. Baturkin, R. Findlay, C. Grimm, J.-T. Grundmann, C. Hobbie, E. Ksenik, C. Lange, K. Sasaki, M. Schlotterer, M. Talapina, N. Termtanasombat, E. Wejmo, L. Witte, M. Wrasmann, G. Wübbels, C. Rößler, J. and Ziach, J. Biele, C. Krause, S. Ulamec, M. Lange, O. Mierheim, J. Lichtenheldt, M. Maier, J. Reill, H.-J. Sedlmayr, P. Bousquet, A. Bellion, O. Bompis, C. Cenac-Morthe, M. Deleuze, S. Fredon, E. Jurado, E. Canalias, R. Jaumann, J.-P. Bibring, K. H. Glaßmeier, M. Grott, L. Celotti, F. Cordero, J. Hendrikse, and T. Okada, “MASCOT - The Mobile Asteroid Surface Scout onboard the HAYABUSA2 Mission,” in *Space Science Reviews, Volume 1 / 1962 - Volume 199 / 2016*, Springer, April 2016.
- [5] A. Wedler, B. Rebele, J. Reill, M. Suppa, H. Hirschmüller, C. Brand, M. Schuster, B. Vodermayer, H. Gmeiner, A. Maier, B. Willberg, K. Bussmann, F. Wappeler, and M. Hellerer, “LRU - Lightweight Rover Unit,” in *Proc. of the 13th Symposium on Advanced Space Technologies in Robotics and Automation (ASTRA)*, May 2015.
- [6] M. Maier, M. Chalon, J. Reill, and H.-J. Sedlmayr, “Highly integrated, radiation-hardened, motor controller with phase current measurement,” in *14th Symposium on Advanced Space Technologies in Robotics and Automation (ASTRA)*, ESA/ESTEC, Noordwijk, Netherlands, June 2017.
- [7] T. Instruments, “Product information on company website,” <http://www.ti.com/product/DRV8332>, 2017.
- [8] DARPA, “Defense advanced research projects agency, institutional website,” <https://www.darpa.mil/>, 2017.
- [9] NRL, “U.s. naval research laboratory, insitutional website,” <https://www.nrl.navy.mil/>, 2017.
- [10] SSL, “Space systems loral, insitutional website,” <https://www.sslmda.com/>, 2017.
- [11] ESA, “Space environment information system,” [www.spenvis.oma.be](http://www.spenvis.oma.be), 2017.
- [12] S. M. Seltzer, “Updated calculations for routine space-shielding radiation dose estimates: Shieldose-2,” NIST Publication NISTIR 5477, Gaithersburg, MD., 1994.
- [13] G. P. e. a. Ginet, “Ae9, ap9 and spm: New models for specifying the trapped energetic particle and space plasma environment,” DOI: 10.1007/s11214-013-9964-y, 2013.
- [14] SPENVIS, “Documentation of the used models and their implementation,” <https://www.spenvis.oma.be/help/background/flare/flare.html>, 2017.
- [15] ESA, “Single event effects test method and guidlines,” in *ESCC Basic Specification No. 25100*, ESA/ESTEC, Noordwijk, Netherlands, October 2014.
- [16] ——, “Total dose steady-state irradiation test methon,” in *ESCC Basic Specification No. 22900*, ESA/ESTEC, Noordwijk, Netherlands, June 2016.
- [17] ——, “Recommendations on the use of the escc specification system for the evaluation and procurement of unqualified components,” in *ESCC Basic Specification No. 23100*, ESA/ESTEC, Noordwijk, Netherlands, February 2014.
- [18] ESCC, “European space components coordination,” <https://spacecomponents.org/>, 2017.
- [19] E. Requirements and S. Division, “Commercial electrical, electronic and electromechanical (eee) components,” in *ECSS-Q-ST-60-13C*, ESA/ESTEC, Noordwijk, Netherlands, October 2013.
- [20] ECSS, “European cooperation for space standardization,” <http://ecss.nl/>, 2017.
- [21] H. Z. B. Wannsee, “Cobalt-60 source,” [http://www.helmholtz-berlin.de/angebote/tt-industrie/methoden/kobalt/index\\_de.html](http://www.helmholtz-berlin.de/angebote/tt-industrie/methoden/kobalt/index_de.html), 2017.
- [22] U. of Jyvaskyla, “Radiation effects facility - RADEF,” <https://www.jyu.fi/fysiikka/en/research/accelerator/radef/facility>, 2017.